

## Observation of Departure from Nucleate Boiling under different flow rates

Byong Guk Jeon<sup>a\*</sup>, Moonhee Choi<sup>b</sup>, Dong Hoon Kam<sup>a</sup>, Sang-Ki Moon<sup>a</sup>

<sup>a</sup>Korea Atomic Energy Research Institute, 989-111 Daedeokdaero, Yuseong, Daejeon, 34057, Korea

<sup>b</sup>Pohang University of Science and Technology, 77 Cheongam-Ro, Nam-Gu, Pohang, 37673, Korea

\*Corresponding author: bgjeon@kaeri.re.kr

### 1. Introduction

Departure from nucleate boiling (DNB) is one of main limiting phenomena in the safety of a nuclear reactor. For the prediction of critical heat flux at DNB, several mechanistic models have been suggested. Well-known mechanistic models include hydrodynamic instability, macrolayer dryout, hot/dry spot, and interfacial lift-off model [1]. These mechanistic models were verified or abandoned through advanced measurement techniques.

Among the techniques, total reflection technique enabled observation of dry patch behaviors under pool and flow boiling. At high heat flux, a coalesced massive bubble is generated with its dry patch below. When the bubble departs from the boiling surface, it leaves its bottom remnant part. As a result, the residual dry patch under the remnant bubble expands again, leading to DNB [2-4]. Another technique, i.e. thermal observation on the dry patch using an infrared (IR) camera, was utilized as well [5]. From it, the heat flux profile as function of superheat was obtained and used to prove the continuum percolation model for boiling crisis [6]. In our research, we examined the phenomenon of DNB using aforementioned techniques under different flow rates

### 2. Methods and Results

#### 2.1 Experiment Loop Setup

We set up a water flow loop under atmospheric pressure (Fig. 1). The loop includes a rectangular test section comprised of an ITO (Indium tin oxide) heater coated on a sapphire substrate. The cross sectional size of the flow channel was 1.5 cm by 1.5 cm and the ITO heater was 1 cm wide and 12 cm long. The long length of the ITO heater enabled development of coagulated bubbles upstream of the DNB location.

To observe the boiling surface, two high-speed cameras and one IR camera were installed with lighting systems (Fig. 2). One high-speed camera recorded the side view of the channel focusing on the bubble structures. The other high-speed camera recorded total internal reflection images. The IR camera recorded the radiation counts on the ITO heater surface. Images from IR camera were synchronized spatially and temporally. The spatial resolution and frequency of measurement were 74  $\mu\text{m}$  and 1.5 kHz, respectively.

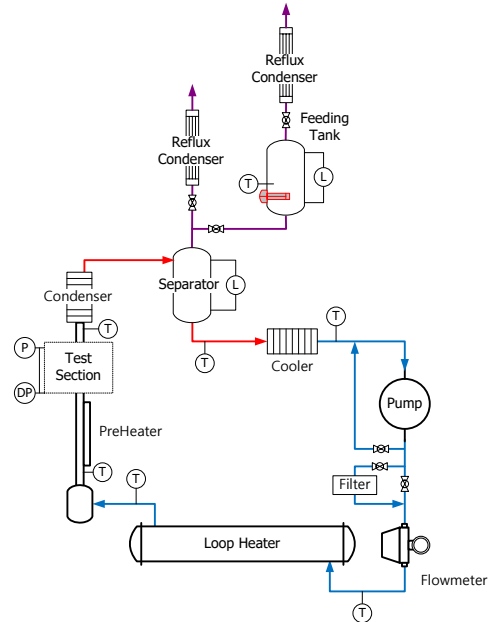


Fig. 1. Schematic for the DNB test loop

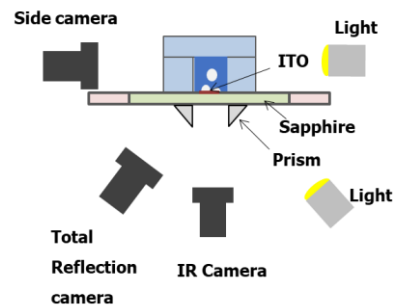


Fig. 2. Arrangement of cameras around the test section

#### 2.2 Observation of DNB under different flow

The CHF values at different flowrates are given in Figure 3. The CHF values increased from 1500  $\text{kW/m}^2$  to 1700  $\text{kW/m}^2$  as the flow rate increased from 250  $\text{kg/m}^2\text{s}$  to 1000  $\text{kg/m}^2\text{s}$ . In the test, the inlet temperature was 95  $^\circ\text{C}$  and the pressure was 1 atm.

Images from two high speed cameras and IR camera at DNB are shown in Figure 4. From left, full side-view (11 cm length), full total reflection view (11 cm length), magnified side-view (7 cm length, corresponding to the red rectangle of the full view), magnified total reflection view (7 cm length), temperature profile (7 cm length) are disposed.

In all tests, slug flow was observed. Elongated bubbles, or vapor slugs, were formed intermittently by coagulation of bubbles. Passage of a vapor slug enabled formation and growth of a dry patch once the microlayer under the slug was evaporated.

In the magnified total reflection image, the green, yellow, and pink contours mean 140 °C, 150 °C, and 160 °C. The boundary temperature of dry patches was roughly 150 °C for all cases.

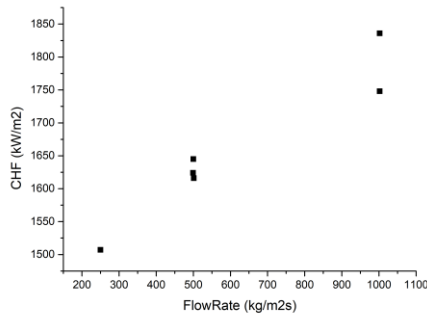


Fig. 3. CHF at different flowrates

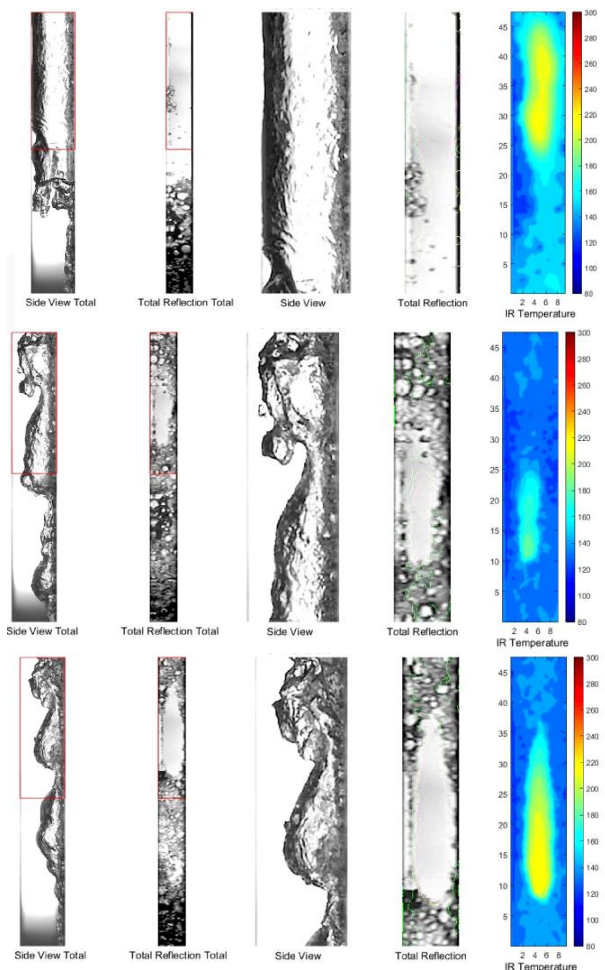


Fig. 4. Images from HSC and IR Camera at DNB

(From left, full side-view, full total reflection view, magnified side-view, magnified total reflection view, temperature profile)

(From top, 250 kg/m²s (CHF 1507 kW/m²), 500 kg/m²s (CHF 1624 kW/m²), 1000 kg/m²s (CHF 1836 kW/m²))

Relatively larger elongated bubbles and dry patches were formed when the flowrate was low, which led to smaller CHF.

### 3. Conclusions

To explore the mechanism of departure from nucleate boiling, optical visualization - side view, and total reflection- and IR thermometry were utilized. These techniques were applied to a DNB test loop, where upward flow was made at different flow rates. As a result, we observed the formation of dry patches with its periphery temperature of 150 °C. Larger elongated bubbles and dry patches were observed under lower flow.

### Acknowledgment

This work was supported by the National Research Foundation of Korea (NRF) grant funded by the Korea government (MSIP) (No. 2017M2A8A4015023).

### REFERENCES

- [1] G. Liang, I. Mudawar, Pool boiling critical heat flux (CHF) – part 1: review of mechanisms, models, and correlations, *International Journal of Heat and Mass Transfer*, Vol. 117, pp. 1352-1367, 2018
- [2] I. C. Chu, H. C. NO, et al., Observation of critical heat flux mechanism in horizontal pool boiling of saturated water, *Nuclear Engineering and Design*, Vol. 279, pp. 189- 199, 2014.
- [3] S. H. Kim, I. C. Chu, et al., Mechanism study of departure of nucleate boiling on forced convective channel flow boiling, *International Journal of Heat and Mass Transfer*, Vol. 126, pp. 1049-1058, 2018
- [4] M. H. Choi, I. C. Chu, et al., Direct observation of rewetting failure mechanism at CHF under different subcooled flows, *International Journal of Heat and Mass Transfer*, Vol. 163, 120465, 2020
- [5] T. G. Theofanous, T. N. Dinh, et al., The boiling crisis phenomenon Part II: dryout dynamics and burnout, *Experimental Thermal and Fluid Science*, Vol. 26, pp. 793-810, 2002.
- [6] G.-Y. Su, C. Wang, et al. Investigation of flow boiling heat transfer and boiling crisis on a rough surface using infrared thermometry, *International Journal of Heat and Mass Transfer*, Vol. 160, 120134, 2020